

Graphitic carbon nitride photocatalysis: the hydroperoxyl radical role revealed by kinetic modelling

Inmaculada Velo-Gala^{a*}, André Torres-Pinto^a, Cláudia G. Silva^a, Bunsho Ohtani^b, Adrián M.T. Silva^a, Joaquim L. Faria^a

^a*Laboratory of Separation and Reaction Engineering - Laboratory of Catalysis and Materials (LSRE-LCM), Faculdade de Engenharia, Universidade do Porto, Porto 4200-465, Portugal*

^b*Institute for Catalysis, Hokkaido University, Sapporo 001-0021, Japan*

*Corresponding author e-mail address: invega@fe.up.pt

Supplementary Material

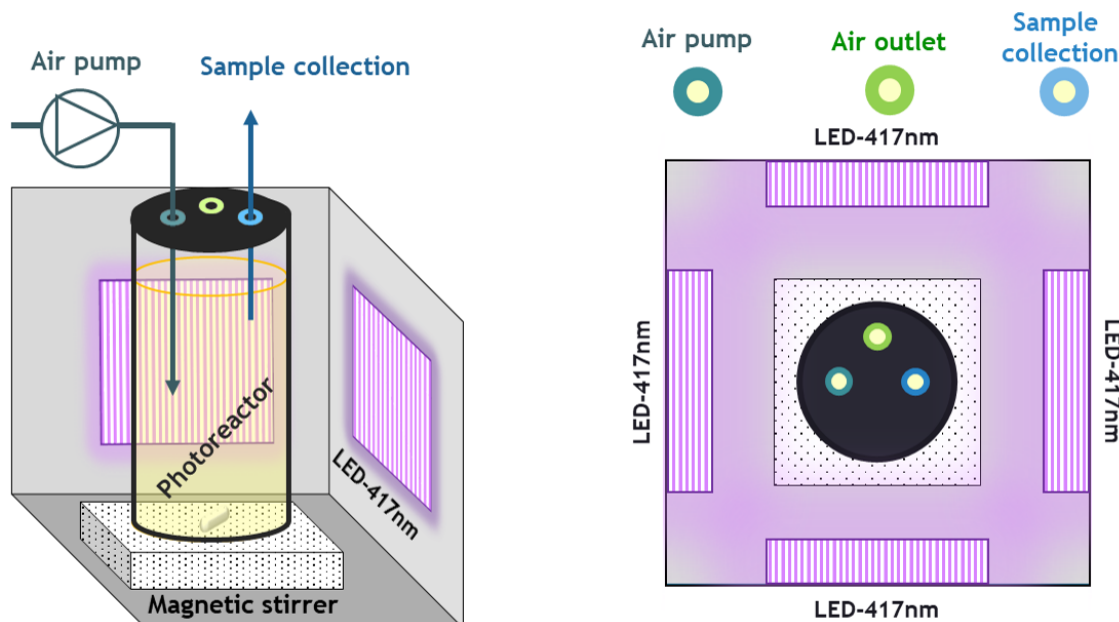


Figure S1. Scheme of the photocatalytic system with a three-dimensional view (left) and a top-view cross-section (right).

Table S1. Kintecus model reactions.

Reactions and rate constants included in the kinetic model

Reaction no.	Reactions in LED-417/GCN	Rate constant $k, (\text{M}^{-1}\cdot\text{s}^{-1})$	Reference
R1	$\text{g-C}_3\text{N}_4 + h\nu \rightarrow 3\text{e}^- + 3\text{h}^+$	3.72	This study
R2	$\text{e}^- + \text{h}^+ \rightarrow \text{recombination}$	1.00×10^{17}	This study
R3	$\text{h}^+ + \text{H}_2\text{O} \rightarrow \text{HO}^\bullet + \text{H}^+$	$\leq 1.00 \times 10^3$	This study
R4	$\text{h}^+ + \text{H}_2\text{O} \rightarrow \frac{1}{2}\text{O}_2 + \text{H}^+$	1.00×10^3	This study
R5	$\text{h}^+ + \text{H}_2\text{O}_2 \rightarrow \text{O}_2 + 2\text{H}^+$	$1.70\text{-}2.50 \times 10^9$	This study
R6	$\text{h}^+ + \text{H}_2\text{O}_2 \rightarrow \text{HO}_2^\bullet + \text{H}^+$	$2.00\text{-}3.00 \times 10^9$	This study
R7	$\text{h}^+ + \text{C}_6\text{H}_5\text{OH} \rightarrow \text{C}_6\text{H}_5\text{O}^\bullet + \text{H}^+$	$1.00\text{-}2.00 \times 10^{10}$	This study
R8	$\text{C}_6\text{H}_5\text{OH} + \text{HO}^\bullet \rightarrow \text{C}_6\text{H}_5\text{O}^\bullet + \text{H}_2\text{O}$	6.00×10^8	[1]
R9	$\text{C}_6\text{H}_5\text{OH} + \text{HO}^\bullet \rightarrow \text{C}_6\text{H}_5(\text{OH})_2$	1.35×10^{10}	[2]
R10	$\text{C}_6\text{H}_5\text{OH} + \text{O}_2^\bullet \rightarrow \text{C}_6\text{H}_5\text{O}^- + \text{HO}_2^\bullet$	5.80×10^2	[3]
R11	$\text{C}_6\text{H}_5\text{OH} + \text{HO}_2^\bullet \rightarrow \text{C}_6\text{H}_5\text{O}^- + \text{H}_2\text{O}_2$	2.70×10^3	[4]
R12	$\text{C}_6\text{H}_5\text{O}^\bullet + \text{O}_2 \rightarrow \text{C}_6\text{H}_4\text{O} + \text{HO}_2^\bullet$	1.30×10^5	[5]
R13	$\text{C}_6\text{H}_5\text{O}^\bullet + \text{O}_2^\bullet \rightarrow \text{C}_6\text{H}_5\text{O}^- + \text{O}_2$	2.00×10^9	[6]
R14	$\text{C}_6\text{H}_5\text{O}^- + \text{HO}_2^\bullet \rightarrow \text{C}_6\text{H}_5\text{O}^\bullet + \text{HO}_2^-$	1.00×10^9	[7]
R15	$\text{C}_6\text{H}_5\text{O}^- + \text{O}^\bullet + \text{H}^+ \rightarrow \text{C}_6\text{H}_5\text{O}^\bullet + \text{HO}^-$	6.50×10^8	[8]
R16	$\text{C}_6\text{H}_5\text{O}^- + \text{HO}^\bullet \rightarrow \text{OHC}_6\text{H}_5\text{O}^-$	9.60×10^9	[9]
R17	$\text{C}_6\text{H}_5(\text{OH})_2 + \text{e}^- \rightarrow \text{C}_6\text{H}_5\text{O}^\bullet + \text{H}_2\text{O}$	1.00×10^9	[10]
R18	$\text{C}_6\text{H}_5(\text{OH})_2 \rightarrow \text{C}_6\text{H}_4(\text{OH})_2 + \text{H}^+$	8.00×10^5	[11]
R19	$\text{C}_6\text{H}_5(\text{OH})_2 + \text{O}_2 \rightarrow \text{C}_6\text{H}_5(\text{OH})_2\text{O}_2^\bullet$	1.20×10^9	[11]
R20	$\text{C}_6\text{H}_5(\text{OH})_2\text{O}_2^\bullet \rightarrow \text{C}_6\text{H}_4(\text{OH})_2 + \text{HO}_2^\bullet$	1.30×10^5	[11]
R21	$\text{C}_6\text{H}_4(\text{OH})_2 + \text{O}_2^\bullet \rightarrow \text{H}_2\text{O}_2 + \text{C}_6\text{H}_4\text{O}_2$	1.70×10^7	[12]
R22	$\text{C}_6\text{H}_4(\text{OH})_2 + \text{HO}_2^\bullet \rightarrow \text{H}_2\text{O}_2 + \text{C}_6\text{H}_5\text{O}_2^\bullet$	1.00×10^3	[13]
R23	$\text{C}_6\text{H}_4(\text{OH})_2 + \text{HO}^\bullet \rightarrow \text{C}_6\text{H}_4(\text{OH})_3$	1.00×10^{10}	[14]
R24	$\text{C}_6\text{H}_4(\text{OH})_2 + \text{O}_3 \rightarrow \text{product}$	1.50×10^6	[15]
R25	$\text{C}_6\text{H}_4\text{O} + \text{HO}^\bullet \rightarrow \text{C}_6\text{H}_5\text{O}^\bullet + \text{O}^\bullet$	1.00×10^{10}	[14]
R26	$\text{C}_6\text{H}_4\text{O}_2 + \text{e}^- \rightarrow \text{C}_6\text{H}_4\text{O}_2^\bullet$	2.30×10^{10}	[16]
R27	$\text{C}_6\text{H}_4\text{O}_2 + \text{HO}^\bullet \rightarrow \text{C}_6\text{H}_4\text{O}_2(\text{OH})^\bullet$	1.20×10^9	[17]

R28	$C_6H_4O_2 + O_2^{\bullet-} \rightarrow O_2 + C_6H_4O_2^{\bullet-}$	9.00×10^8	[18]
R29	$C_6H_5O_2^{\bullet} + C_6H_5O_2^{\bullet} \rightarrow C_{12}H_8(OH)_2 + O_2$	1.10×10^9	[19]
R30	$e^- + O_2 \rightarrow O_2^{\bullet-}$	1.90×10^{10}	[16]
R31	$O_2 + 2e^- + 2H^+ \rightarrow H_2O_2$	1.90×10^{10}	[20]
R32	$O_2^{\bullet-} + H^+ \rightarrow HO_2^{\bullet}$	7.20×10^{10}	[21]
R33	$HO_2^{\bullet} \rightarrow O_2^{\bullet-} + H^+$	1.60×10^{-5}	[7]
R34	$HO_2^{\bullet} + H^+ \rightarrow H_2O_2$	1.00×10^{10}	[7]
R35	$HO_2^{\bullet} + O_2^{\bullet-} \rightarrow O_2 + HO_2^-$	9.70×10^7	[7]
R36	$H^+ + HO^- \rightarrow H_2O$	1.00×10^{11}	[22]
R37	$H_2O \rightarrow H^+ + HO^-$	1.30×10^{-3}	[22]
R38	$HO_2^{\bullet} + HO_2^{\bullet} \rightarrow O_2 + H_2O_2$	3.40×10^7	[10]
R39	$HO_2^- + H^+ \rightarrow H_2O_2$	5.00×10^{10}	[22]
R40	$HO_2^- + O^{\bullet-} \rightarrow HO^- + O_2^{\bullet-}$	4.00×10^8	[10]
R41	$H_2O_2 \rightarrow H^+ + HO_2^-$	1.26×10^{-1}	[22]
R42	$H_2O_2 + HO_2^{\bullet} \rightarrow HO^{\bullet} + O_2 + H_2O$	3.00	[23]
R43	$H_2O_2 + 2e^- \rightarrow HO^{\bullet} + HO^-$	9.50×10^9	[16]
R44	$H_2O_2 + O_2^{\bullet-} \rightarrow O_2 + HO^{\bullet} + HO^-$	2.30×10^{-1}	[24]
R45	$HO^{\bullet} + H_2O_2 \rightarrow H_2O + O_2^{\bullet-} + H^+$	2.70×10^7	[10]
R46	$HO^{\bullet} + H_2O_2 \rightarrow HO_2^{\bullet} + H_2O$	2.70×10^7	[10]
R47	$HO^{\bullet} + HO^{\bullet} \rightarrow H_2O_2$	5.20×10^9	[10]
R48	$HO^{\bullet} + HO^- \rightarrow H_2O + O^{\bullet-}$	1.30×10^{10}	[10]
R49	$HO^{\bullet} + HO_2^{\bullet} \rightarrow H_2O + O_2$	7.53×10^9	[25]
R50	$HO^{\bullet} + HO_2^- \rightarrow H_2O + O_2^{\bullet-}$	7.50×10^9	[10]
R51	$HO^{\bullet} + O_2^{\bullet-} \rightarrow O_2 + HO^-$	8.50×10^9	[25]
R52	$HO^{\bullet} + O_3^{\bullet-} \rightarrow HO_2^{\bullet} + O_2^{\bullet-}$	8.50×10^9	[26]
R53	$HO^{\bullet} + O^{\bullet-} \rightarrow HO_2^-$	2.00×10^{10}	[27]
R54	$H_2O + O^{\bullet-} + O_2^{\bullet-} \rightarrow O_2 + 2HO^-$	6.00×10^8	[28]
R55	$H^+ + O^{\bullet-} \rightarrow HO^-$	2.20×10^{10}	[10]
R56	$O^{\bullet-} + H_2O \rightarrow HO^{\bullet} + HO^-$	9.40×10^7	[10]
R57	$O^{\bullet-} + O^{\bullet-} \rightarrow O_2 + 2e^-$	8.40×10^9	[29]
R58	$O^{\bullet-} + O_2 \rightarrow O_3^{\bullet-}$	3.60×10^9	[10]
R59	$O_3^{\bullet-} + O^{\bullet-} \rightarrow 2 O_2^{\bullet-}$	7.00×10^8	[30]

R60	$O_3^{\bullet-} + H^+ \rightarrow O_2 + HO^\bullet$	5.20×10^{10}	[31]
R61	$O_3^{\bullet-} \rightarrow O_2 + O^{\bullet-}$	3.30×10^3	[32]
R62	$h^+ + HO^- \rightarrow HO^\bullet$	---	

Text S1. Theoretical calculation of photocatalysis rate

The photocatalysis rate (k_{photo}) of GCN with a 417 nm LED radiation was calculated as Equations S1-S3.

$$k_{photo} = \frac{r_0}{I_0} \quad (S1)$$

$$r_0 = k_{obs} \cdot C_i \quad (S2)$$

$$k_{obs} = -\ln \frac{C_i - C_f}{C_i} \quad (S3)$$

Where r_0 is the initial rate of the photocatalytic reaction ($M s^{-1}$), I_0 is the incident radiation (Einstein $L^{-1} \cdot s^{-1}$), k_{obs} is the photocatalytic degradation rate of PhOH, C_i is the initial concentration of PhOH, and C_f is the theoretical concentration at one second of reaction calculated as Equation S4. The final reaction time was one second because, in this condition, it is assumed that phenol molecules are only degraded *via* the photocatalytic process over the total number of photons absorbed [33].

$$C_f = \frac{\text{absorbed photons at 1 seg (Einstein}\cdot\text{s}^{-1}) \times \varphi}{\text{volume (L)}} \quad (S4)$$

The absorbed photons are difficult to evaluate in a photocatalytic system due to the absorption, transmission, and scattering of the semiconductor particles. As reported in the literature [34-37], it was calculated considering the reactor geometry (irradiation area) and the molar absorptivity as the number of reactant molecules transformed divided by the number of photons of the light incident inside the reactor. The average apparent quantum efficiency (φ) is the ratio of 90% converted reactant molecules over the photons entering the reactor (Eq. S5) [36, 38, 39].

$$\varphi = \frac{\frac{N_{90}}{t_{90}}}{\frac{I \cdot A}{v \cdot h}} \quad (S5)$$

Where N_{90} are 90% transformed moles at its matching time (t_{90} , 90 seconds), I is the radiation intensity (Einstein $m^{-2} s^{-1}$), A is the number of catalytically active sites estimated

by multiplying the specific surface area (S_{BET} , in $\text{m}^2 \text{ g}^{-1}$) of the catalyst particles and its mass (g), ν is the frequency (c/λ), and h is the Planck constant. In this calculation, the S_{BET} was assumed as $87 \text{ m}^2 \text{ g}^{-1}$ according to our previous work [40].

It must be noted that the BET surface areas suggest the number of adsorption sites, but it does not necessarily represent the number of catalytically active sites. However, this assumption is commonly accepted as a conservative estimation for the active sites when the photocatalytic process depends on the surface characteristics [39, 41].

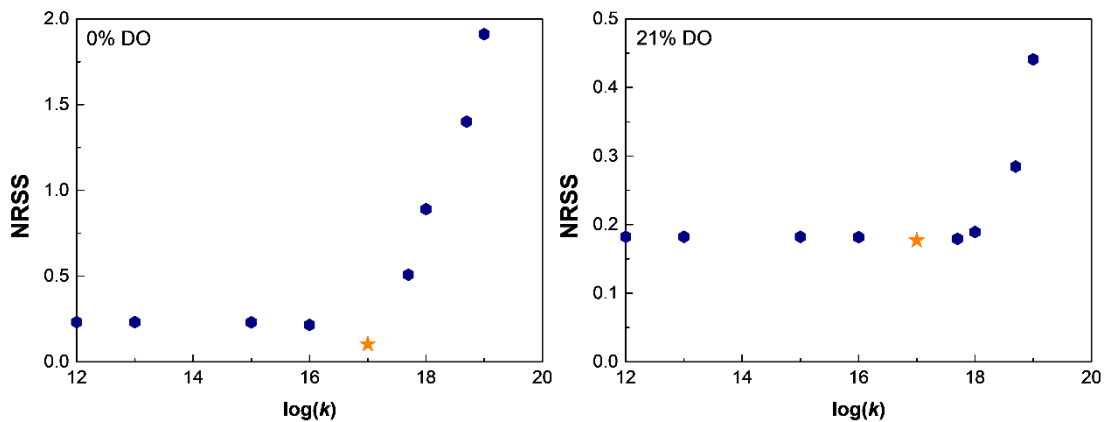
Text S2. Sensitivity analysis

The Normalised Residuals Sum of Squares (NRSS) value represents the average deviation of the resolved model from the experimental data. It is an indicator of the capacity of the model to reproduce the experimental data. The average RSS is defined as Equation S.6:

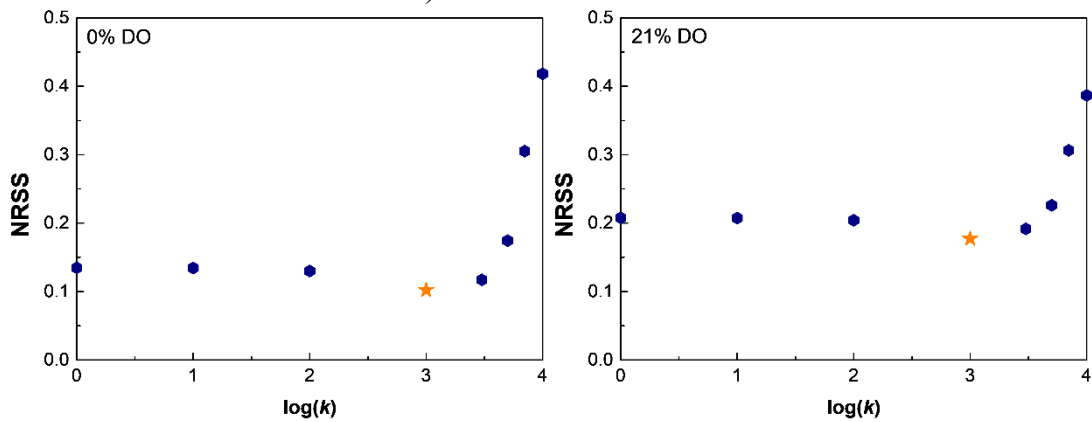
$$\text{NRSS} = \frac{1}{n} \sum_{i=1}^n \frac{|M_i - D_i|}{D_i} \quad (\text{S6})$$

Where M_i is the model response at a given system condition and time, D_i is the experimental data at the same given condition and time, and n is the total number of measured data points over all conditions and time. To analyse the effect of changes on specific rate constant values [42], the NRSS was calculated by running the model while varying one rate constant with all others held fixed at their optimised values. In this case, the D_i is the altered model response at the same condition and time as the control model.

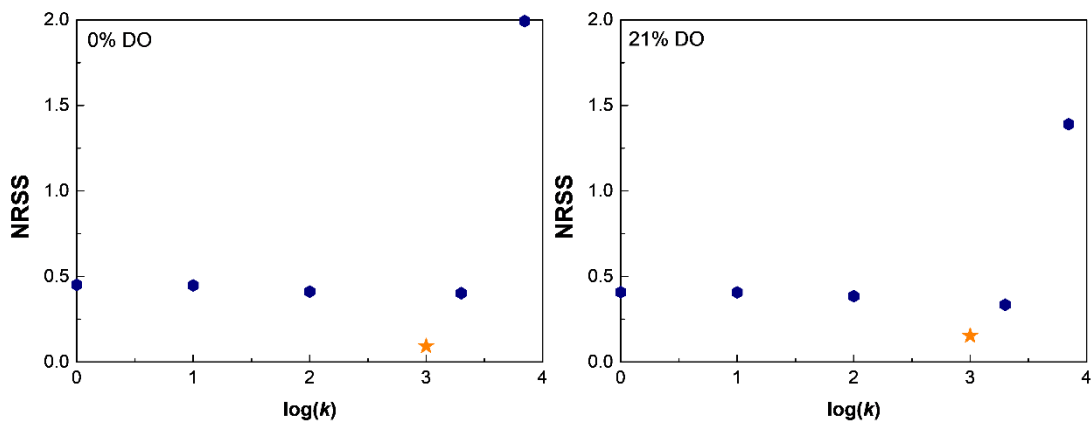
A) $e^- + h^+ \rightarrow$ recombination



B) $h^+ + H_2O \rightarrow HO^\bullet + H^+$



C) $h^+ + H_2O \rightarrow \frac{1}{2}O_2 + H^+$



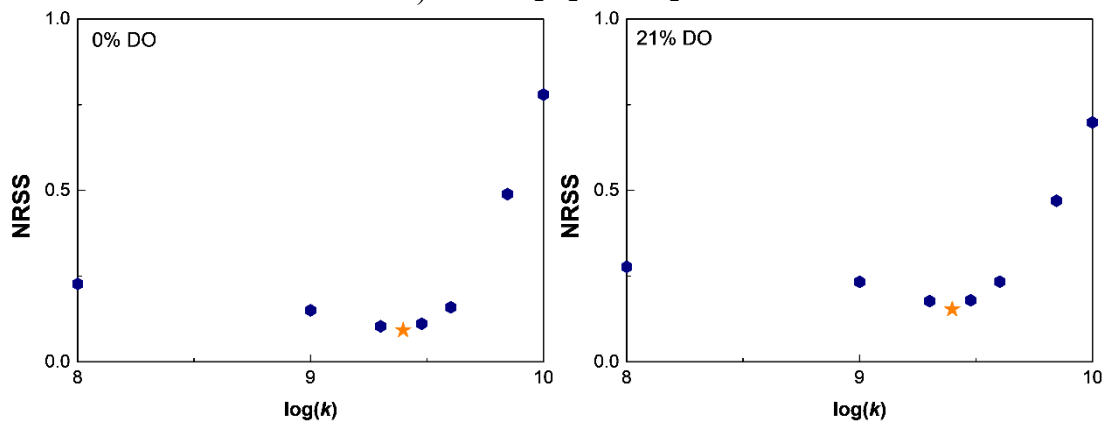
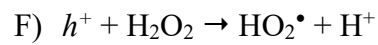
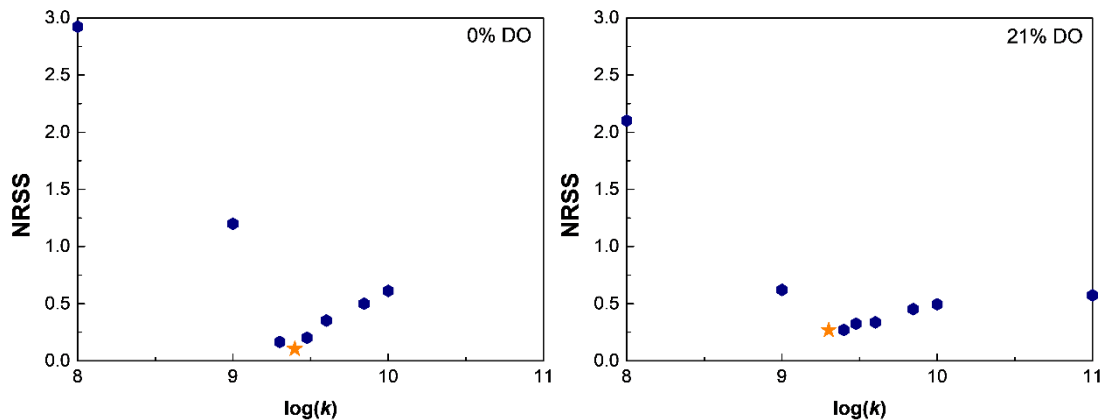
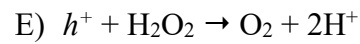
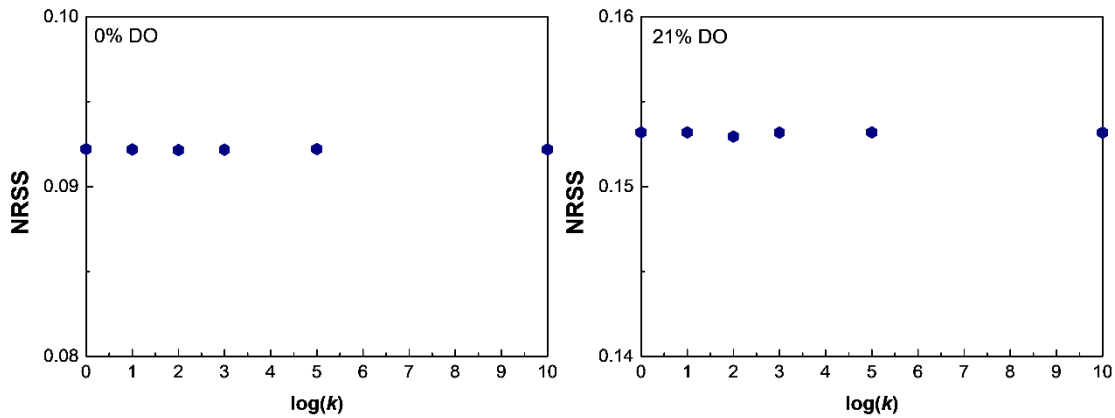
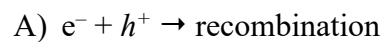
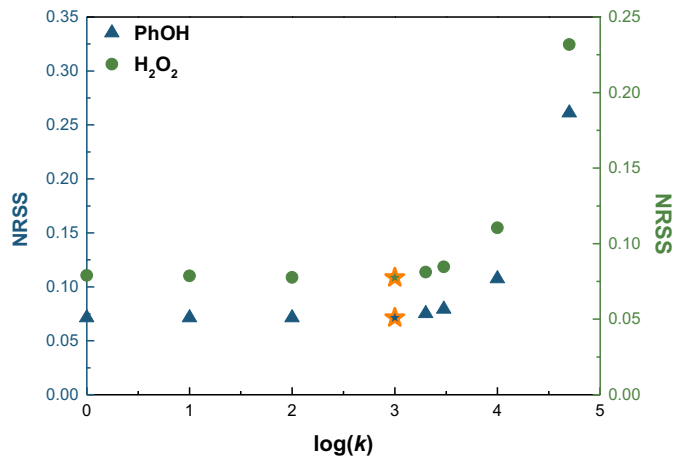
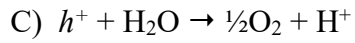
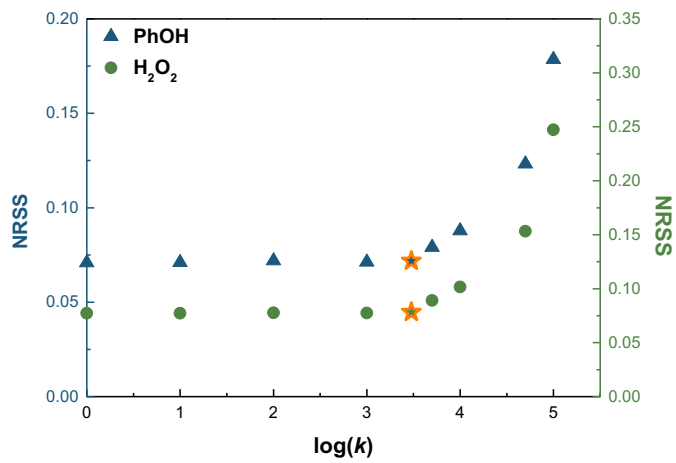
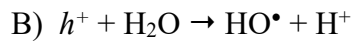
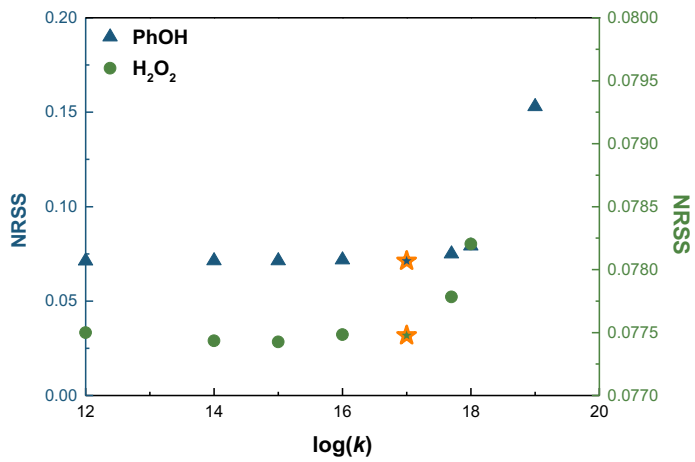
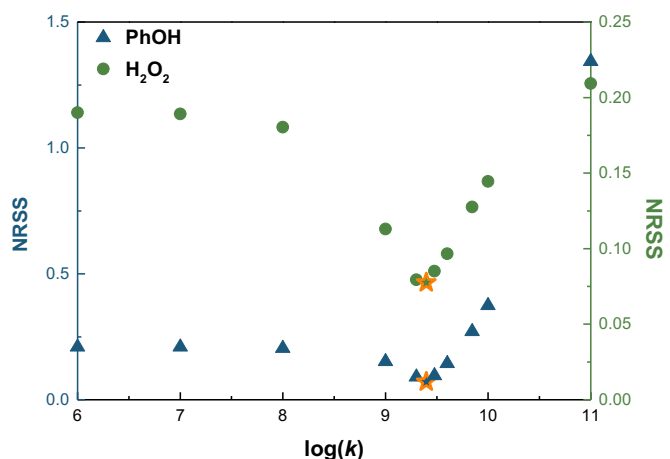
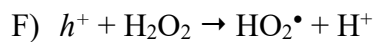
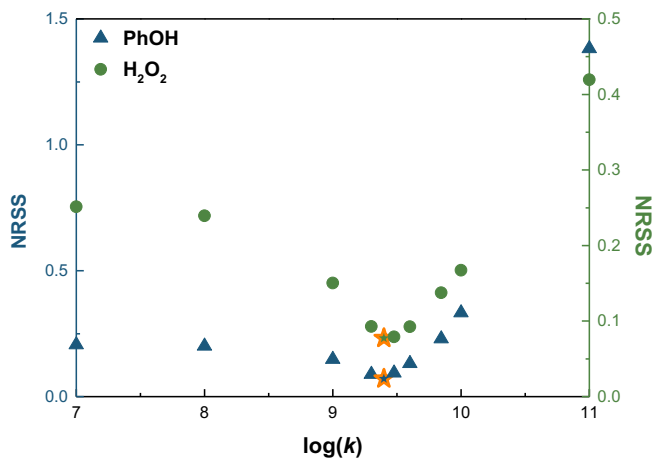
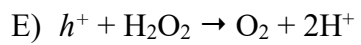
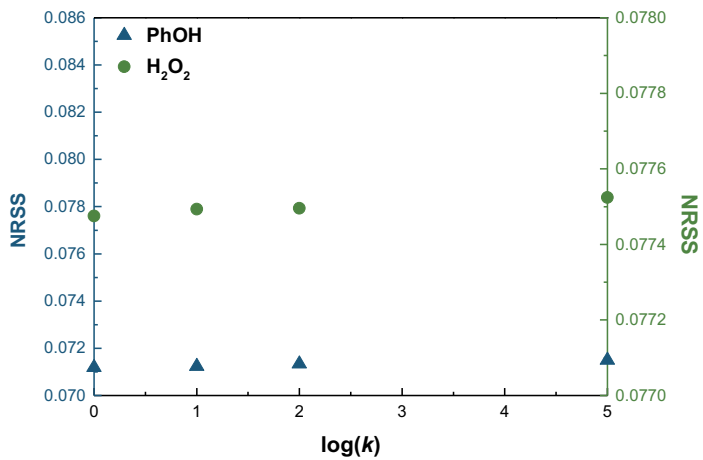


Figure S2. Sensitivity analysis of fitting reaction rate constants: kinetic model of H_2O_2 removal by the LED-417/GCN system. Initial conditions: $\text{pH}_0=6.1$; $[\text{H}_2\text{O}_2]_0=1 \times 10^{-3}$ M.







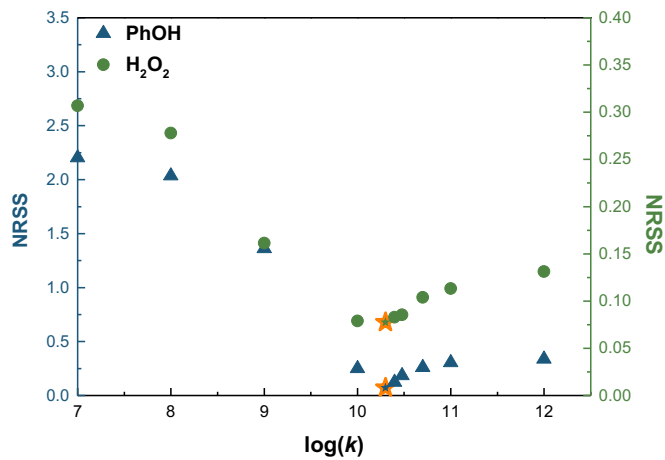


Figure S3. Sensitivity analysis of fitting reaction rate constants: kinetic model of PhOH removal and H_2O_2 generation by the LED-417/GCN system. Initial conditions: $\text{pH}_0=6.1$; $[\text{PhOH}]_0=6.38\times 10^{-4}$ M.

Table S2. Photocatalytic results of PhOH degradation and H_2O_2 generation in the LED-417/GCN system. Experimental initial conditions: $\text{pH}_0=6.1$; $[\text{PhOH}]_0=6.38\times 10^{-4}$ M.

O_2 (%)	PhOH removal $k_{\text{app}} \times 10^2$ (min $^{-1}$)	% PhOH removal (60 min)	H_2O_2 formation rate $k_{\text{app}} \times 10^5$ (min $^{-1}$)	$[\text{H}_2\text{O}_2]/$ mmol L $^{-1}$ (60 min)	Max. $[\text{H}_2\text{O}_2]/$ mmol L $^{-1}$ (time/min)	pH value (180 min)
0	0.05	6.85	0	0	0	8.41
5	0.62	26.5	0.40	0.29	0.66 (180)	7.02
10	1.98	65.0	0.85	0.51	0.74 (150)	5.13
21	2.73	85.6	1.53	0.88	0.90 (120)	4.06
100	6.14	100	2.91	0.96	0.96 (60)	3.83

Table S3. Percentages of PhOH removal depending on the reactive species and the percentage of dissolved oxygen. Data obtained from Kintecus modelling.

%DO	Final degradation (%)	Degradation rate constant $k_{app} \times 10^2 (\text{min}^{-1})$	%D(reactants)				
			%D(h^+) R7	%D(HO^\bullet) R8	%D(HO^\bullet) R9	%D(O_2^\bullet) R10	%D(HO_2^\bullet) R11
0	8.46	0.05	7.98	0.00	0.03	0.00	0.45
5	71.9	0.60	67.2	0.01	0.21	0.00	4.47
10	100	1.80	72.5	0.01	0.27	0.02	27.7
21	100	2.56	62.3	0.01	0.15	0.05	37.5
100	100	5.95	62.2	0.01	0.14	0.05	37.6

Table S4. Percentages of H_2O_2 formation depending on the reaction pathway and the amount (%) of dissolved oxygen (DO). Data obtained from Kintecus modelling.

DO (%)	Max. $[\text{H}_2\text{O}_2]/\text{mmol L}^{-1}$ (time/min)	H ₂ O ₂ formation rate					
		$k_{app} \times 10^5 (\text{min}^{-1})$	%R11	%R21	%R22	%R38	%R39
0	0.04 (180)	0.02	67.0	0.00	0.00	0.50	32.5
5	0.67 (180)	0.38	63.6	0.22	0.08	5.60	30.5
10	0.74 (114)	0.83	35.7	0.25	0.04	50.6	13.4
21	0.97 (88)	2.11	29.4	0.20	0.00	70.4	0.00
100	0.96 (73)	2.39	27.7	0.20	0.00	72.1	0.00

The rest of the reactions (R35, R47, R31) that could form H_2O_2 had no contribution to the model.

Table S5. Percentages of H_2O_2 removal depending on the reaction and the amount (%) of dissolved oxygen (DO). Data obtained from Kintecus modelling.

DO (%)	Degradation (%)	Degradation rate constant $k \times 10^6 (\text{min}^{-1})$				
		% R5	% R6	% R42	% R46	
0	1.27	0	0.55	0.66	0.00	0.00
5	15.9	0	7.22	8.66	0.00	0.00
10	100	2.45	45.3	54.3	0.10	0.30
21	100	2.64	45.4	54.5	0.10	0.00
100	100	2.63	45.4	54.5	0.10	0.00

The rest of the reactions (R43, R45) that could remove H_2O_2 had no contribution to the model.

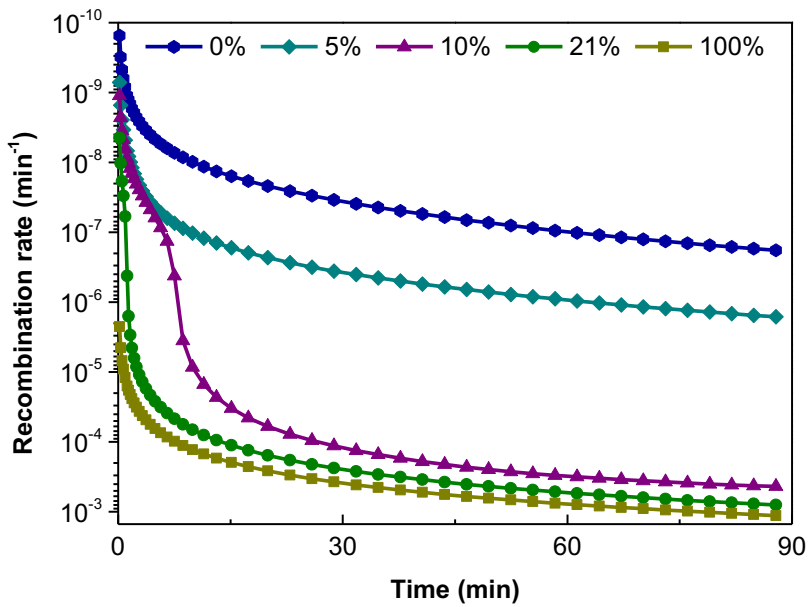


Figure S4. Kinetic model of the recombination e^-/h^+ reaction in the LED-417/GCN system for different percentages of dissolved oxygen (DO).

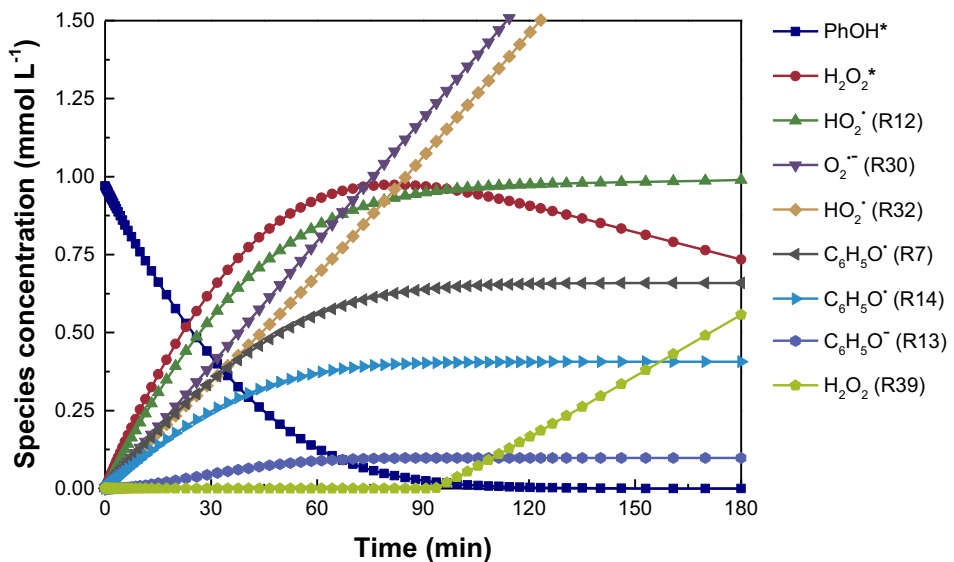


Figure S5. Kinetic modelling for the most relevant reactions involved in H_2O_2 generation. DO 21%. Initial conditions: $\text{pH}_0=6.1$; $[\text{PhOH}]_0= 6.38 \times 10^{-4} \text{ M}$. LED-417/GCN system.

Supplementary characterisation of GCN

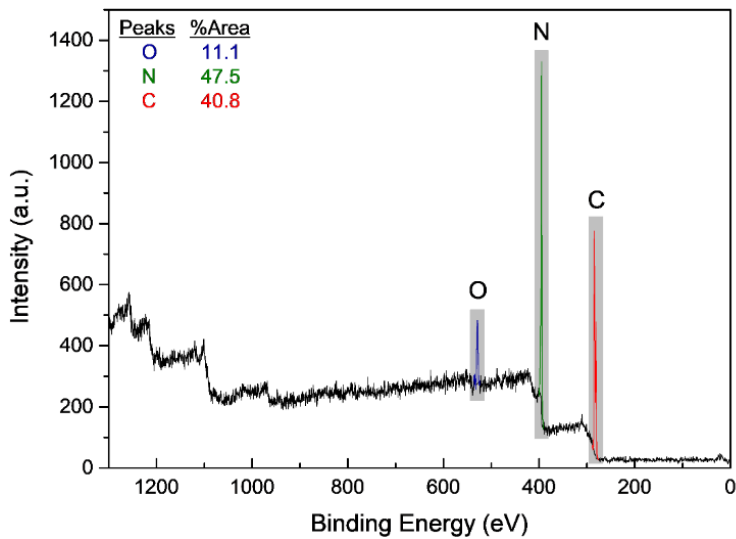


Figure S6. XPS survey spectra of GCN.

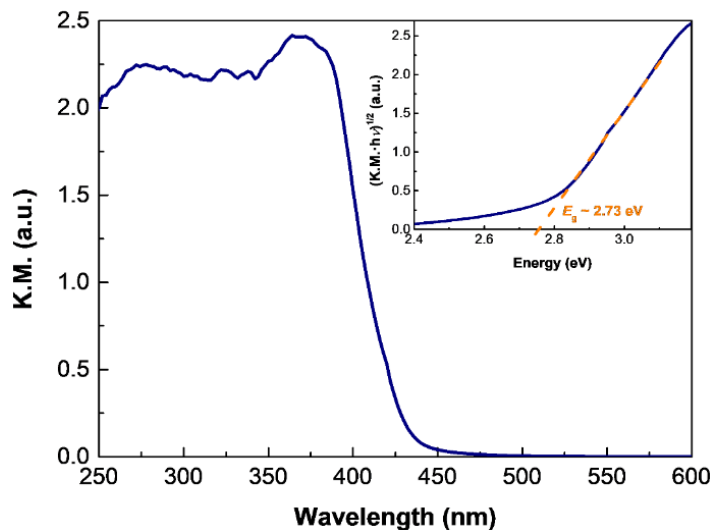


Figure S7. DRS and Tauc plot (inset) of GCN.

Bibliography

- [1] L.M. Dorfman, G.E. Adams, Reactivity of the Hydroxyl Radical in Aqueous Solutions, National Bureau of Standards, U. S. Department of Commerce1973.
- [2] E.J. Land, M. Ebert, *Trans. Faraday Soc.*, 1967, **63**, 1181-1190.
- [3] T. Yasuhisa, H. Hideki, Y. Muneyoshi, *Int. J. Biochem.*, 1993, **25**, 491-494.
- [4] Z. Kozmér, E. Arany, T. Alapi, E. Takács, L. Wojnárovits, A. Dombi, *Radiat. Phys. Chem.*, 2014, **102**, 135-138.
- [5] E. Mvula, M.N. Schuchmann, C. von Sonntag, *J. Chem. Soc., Perkin Trans. 2*, 2001, 264-268.
- [6] M. Jonsson, J. Lind, T. Reitberger, T.E. Eriksen, G. Merenyi, *J. Phys. Chem.*, 1993, **97**, 8229-8233.
- [7] B.H.J. Bielski, D.E. Cabelli, R.L. Arudi, A.B. Ross, *J. Phys. Chem. Ref. Data*, 1985, **14**, 1041-1100.
- [8] P. Neta, R.H. Schuler, *Radiat. Res.*, 1975, **64**, 233-236.
- [9] R.W. Matthews, D.F. Sangster, *J. Phys. Chem.*, 1965, **69**, 1938-1946.
- [10] G.V. Buxton, C.L. Greenstock, W.P. Helman, A.B. Ross, *J. Phys. Chem. Ref. Data*, 1988, **17**, 513-886.
- [11] X.-M. Pan, M.N. Schuchmann, C. von Sonntag, *J. Chem. Soc., Perkin Trans. 2*, 1993, 1021-1028.
- [12] P.S. Rao, E. Hayon, *J. Phys. Chem.*, 1975, **79**, 397-402.
- [13] A.D. Nadezhdin, H.B. Dunford, *Can. J. Chem.*, 1979, **57**, 3017-3022.
- [14] G.E.B. Adams, J.W.; Currant, J.; Michael, B.D., Pulse Radiolysis - Absolute rate constants for the reaction of the hydroxyl radical with organic compounds, Academic Press, New York1965.
- [15] M.D. Gurol, S. Nekouinaini, *Ind. Eng. Chem. Fundam.*, 1984, **23**, 54-60.
- [16] B.H. Milosavljevic, O.I. Micic, *J. Phys. Chem.*, 1978, **82**, 1359-1362.

- [17] G.E. Adams, B.D. Michael, *Trans. Faraday Soc.*, 1967, **63**, 1171-1180.
- [18] C.L. Greenstock, G.W. Ruddock, *Int. J. Radiat. Phys. Chem.*, 1976, **8**, 367-369.
- [19] X. Fang, R. Mertens, C. von Sonntag, *J. Chem. Soc., Perkin Trans. 2*, 1995, 1033-1036.
- [20] E. Bjergbakke, Z.D. Dragarne, K. Sehested, I.G. Dragarne, *Radiochim. Acta*, 1989, **48**, 65-72.
- [21] R.J. Field, R.M. Noyes, D. Postlethwaite, *J. Phys. Chem.*, 1976, **80**, 223-229.
- [22] Y. Yang, J.J. Pignatello, J. Ma, W.A. Mitch, *Environ. Sci. Technol.*, 2014, **48**, 2344-2351.
- [23] W.H. Koppenol, J. Butler, J.W.v. Leeuwen, *Photochem. Photobiol.*, 1978, **28**, 655-658.
- [24] C. Ferradini, J. Foos, C. Houee, J. Puchault, *Photochem. Photobiol.*, 1978, **28**, 697-700.
- [25] A.J. Elliot, G.V. Buxton, *J. Chem. Soc. Faraday Trans.*, 1992, **88**, 2465-2470.
- [26] K. Sehested, J. Holcman, E. Bjergbakke, E.J. Hart, *J. Phys. Chem.*, 1984, **88**, 269-273.
- [27] J. Rabani, M.S. Matheson, *J. Phys. Chem.*, 1966, **70**, 761-769.
- [28] K. Sehested, J. Holcman, E. Bjergbakke, E.J. Hart, *J. Phys. Chem.*, 1982, **86**, 2066-2069.
- [29] G.E. Adams, J.W. Boag, B.D. Michael, L.H. Gray, *Proc. R. Soc. A*, 1966, **289**, 321-341.
- [30] B.L. Gall, L.M. Dorfman, *J. Am. Chem. Soc.*, 1969, **91**, 2199-2204.
- [31] R.E. Buehler, J. Staehelin, J. Hoigne, *J. Phys. Chem.*, 1984, **88**, 2560-2564.
- [32] D. Behar, G. Czapski, *Isr. J. Chem.*, 1968, **6**, 43-51.
- [33] A.E. Cassano, C.A. Martin, R.J. Brandi, O.M. Alfano, *Ind. Eng. Chem. Res.*, 1995, **34**, 2155-2201.

- [34] M.I. Cabrera, O.M. Alfano, A.E. Cassano, *J. Phys. Chem.*, 1996, **100**, 20043-20050.
- [35] O. Carp, C.L. Huisman, A. Reller, *Prog. Solid. State Ch.*, 2004, **32**, 33-177.
- [36] V. Loddo, M. Addamo, V. Augugliaro, L. Palmisano, M. Schiavello, E. Garrone, *AIChE J.*, 2006, **52**, 2565-2574.
- [37] N. Serpone, *J. Photochem. Photobiol. A*, 1997, **104**, 1-12.
- [38] N.J. Peill, M.R. Hoffmann, *Environ. Sci. Technol.*, 1995, **29**, 2974-2981.
- [39] N. Serpone, A. Salinaro, A. Emeline, V. Ryabchuk, *J. Photochem. Photobiol. A*, 2000, **130**, 83-94.
- [40] A. Torres-Pinto, M.J. Sampaio, C.G. Silva, J.L. Faria, A.M.T. Silva, *Appl. Catal. B-Environ.*, 2019, **252**, 128-137.
- [41] B.S. Hugo de Lasa, Miguel Salaices, Photocatalytic Reaction Engineering - Chapter 6: The Energy Efficiency Factors in Photocatalytic Processes, 1 ed., Springer US2005.
- [42] A.L. Rose, T.D. Waite, *Environ. Sci. Technol.*, 2002, **36**, 433-444.